coatings

MDPI

Article

Surface Erosion of Low-Current Reed Switches

Igor A. Zeltser [1,2], Aleksey S. Karpov [1], Evgeny N. Moos [3], Nikolay B. Rybin [4] and Alexander B. Tolstoguzov [2,4,5,*]

1 Ryazan Metal Ceramics Instrumentation Plant Joint Stock Company (RMCIP JSC), Novaya Str. 51B, 390027 Ryazan, Russia; zeltseria@rmcip.ru (I.A.Z.); karpovas@rmcip.ru (A.S.K.)
2 Limited Liability Company "Ecton", Innovation Center Skolkovo, Lugovaya Str. 4/1, 143026 Moscow, Russia
3 Physical Department, Yesenin Ryazan State University, Svoboda Str. 46, 390000 Ryazan, Russia; e_moos@mail.ru
4 Department of Nano- and Microelectronics, Ryazan State Radio Engineering University, Gagarin Str. 59/1, 390005 Ryazan, Russia; nikolay.rybin@yandex.ru
5 Centre for Physics and Technological Research (CeFITec), Departamento de Física da Faculdade de Ciências e Tecnologia, Universidade Nova de Lisboa, 2829-516 Caparica, Portugal
* Correspondence: a.tolstoguzov@fct.unl.pt; Tel.: +7-960-577-7900

Academic Editor: Mark D. Soucek
Received: 18 April 2017; Accepted: 31 May 2017; Published: 3 June 2017

Abstract: The erosion model of the surface coatings of reed switches considering different physicochemical processes occurring on the contact surfaces and inside the inter-electrode gap was proposed. According to that, the discrete electron avalanche (*ecton*) introduced in the explosive electron emission theory by Mesyats is considered as the main motive force responsible for the surface modification and mass transfer of materials in the course of breaking/shorting of the contacts. By means of SEM imaging and energy dispersive X-ray microanalysis of the contact surfaces after various numbers of switching cycles, the energy threshold of the *ecton* generation defining the erosion stability of the coatings was found to be proportional to the specific sublimation and ionization energies of coating materials. It has been shown that the total erosion of the coatings on the working surface of the contacts after the commutation test possess the resultant character; i.e., the specificities of erosion occurring after each commutation event are characteristic for the whole of the commutation test. In further development of our model, we suggested that a few monolayers of metals (or alloys) with low ionization potential deposited on the main coatings can improve the erosion stability of contacts.

Keywords: reed switch; surface erosion; nitrogen-containing coatings; electric current commutation; scanning electron microscopy; energy dispersive X-ray microanalysis; criterion of erosion stability

1. Introduction

The surface erosion of magnetically operated hermetical contacts (reed switches or RS) [1] occurring under the commutation of electrical current is similar in many respects to the processes taking place in the course of explosive electron emission, arc and spark discharges [2,3], electrical discharge machining and doping [4,5], surface modification by pulse discharges [6–9], and high-intensity ion, plasma, and laser irradiation of materials [10,11]. There are currently no generally recognized models explaining these processes, since they occur under non-equilibrium conditions, in limited volumes, and during short time intervals.

It is known (e.g., [12,13] and references therein) that the erosion stability of materials depends on their thermophysical characteristics such as heat capacity and conductivity, melting point, etc. However, the criteria of erosion stability resting upon these characteristics (e.g., the Palatnik's criterion [14]) cannot be considered as universal because they allow for the processes occurring

only in liquid and vapor phases. Erosion in solid phase, mass transfer initiated by plasma, electron, and ion fluxes are not considered in these criteria. At the same time, the prevention of surface erosion under the influence of these fluxes not only has great scientific importance, but can also contribute to the development of leading-edge technologies for reactor shielding, protective coatings of spacecraft, thin films, and the production of multilayer structures in micro- and nanoelectronics, etc.

Reed switches are electromechanical devices possessing high mechanical and radioactive stability, low electrical resistance, and providing total galvanic isolation of the switched circuits without electrical consumption in standby mode. RS can operate within a wide temperature range (from −60 °C to 150 °C) in a polluted and corrosive atmosphere with very high reliability. Further, these devices are used in the development of new technologies in various important fields such as telecommunications, aerospace, military, scientific and medical equipment, and in household appliances. In the course of switching cycles (the number of which can reach 10^9), complex physicochemical and electric discharge processes can occur on the surface and near-surface region of the contacts, leading to their damage and service failure mainly due to the surface erosion. From this point of view, an understanding of the erosion behavior can increase the reliability and operating life of reed switches. From a scientific point of view, reed switches can be considered as controllable modeling systems suitable for the development and verification of the criteria of the erosion stability of materials.

Initially, the formation of liquid metal jumpers (bridges) under the commutation of electrical current greater than 1–10 mA was considered as the primary reason for the surface erosion of reed switches. Mesyats [2,3] has refined this by introducing the discrete electron avalanche (named *ecton*), which is born during the explosion of liquid metal bridges. *Ecton* can be regarded as the main motive force of mass transfer under breaking/shorting of the contacts. However, in his explosive electron emission theory, the modification of contact surfaces and the formation of surface relief—craters, holes, humps, and other features—during the commutation of electrical current had been not paid sufficient attention in spite of the great importance of these processes for the development of the criteria of erosion stability.

In the present work, we discuss and explain the experimental results obtained for low-current reed switches with nitrogen-containing iron/nickel coatings. We have conducted a detailed study of mass transfer and materials redistribution on the surface of reed switches during the commutation of electrical circuits with an active load. As a result, the criterion of erosion stability considering different processes on the contact surfaces and the inter-electrode gap of reed switches has been developed and compared with the factor of electroerosion machinability of the contact materials.

2. Materials and Methods

We studied a prototype model (Figure 1) 14 mm in length manufactured at RMCIP JSC (Ryazan, Russia) on the basis of commercial MKA-14103 low-current reed switches produced at the same company [1]. These are normally open RS applicable to the commutation of DC and AC electrical circuits with the maximal values of 1 A, 200 V, 10 W, and 10 kHz. The magnetomotive force (the operating ampere-turns) does not reach lower than 4 A, and the resetting ratio ranges between 0.35 and 0.9. The main difference of the prototype against a standard device is the absence of the gold-ruthenium electrodeposited coatings on the contact surfaces. Instead of those, nitrogen-containing iron/nickel coatings were fabricated directly in reed switches using pulsed ion-plasma treatment [6–9].

Figure 1. External view of a reed switch (RS) prototype model studied in this work. Its overall dimension is 44.7 mm, the bulb's length and diameter are 14.2 mm and 2.3 mm, respectively.

The contacts (blades) were pressed with vacuum-melt permalloy (Ni 52 wt %, Fe 48 wt %) wires by Dilaton™, degreased, and annealed in hydrogen atmosphere. When sealing the reed switch, the bulb

was filled with dry nitrogen under the pressure of ca. 40 kPa with the purity of 99.999% and the dew point not higher than −63 °C.

The gap between parallel blades was 30 μm, and the overlapping (contact or working) region was 400 μm in length and 680 μm in width. After sealing, the nitrogen-containing coatings were fabricated directly in reed switches. The voltage pulses with amplitude of ca. 2 kV, duration of 2–20 μs, and frequency of 1 kHz were nearly rectangular, and they followed in groups (packets). Each particular packet consisted of five pulses, whose polarity changed at a frequency of 50 Hz. The duration of the single ion-plasma treatment was 30 s with 30 s pause between each single treatment, and the total number of such treatments was as high as 30. In that case, the reed switch is considered as a simple diode system, where blades act as electrodes (cathode and anode), and the glass bulb filled with nitrogen serves as a working chamber (for detail, see [6–9] and references cited therein).

The commutation (switchgear) tests were carried out with 0.04–0.8 A, 24 V, 50 Hz of sinusoidal voltage by using an active load. The number of switching cycles ranged up to 10^6. It is known [15] that the operating ampere-turns of reed switches depends on switchgear current, and an increase of this current can decrease the contact force. However, this effect has a significant influence only when the switchgear current becomes higher than 1 A. The morphology and uniformity of the surface coatings were determined before and after the commutations by a JEOL JSM-6610LV (Tokyo, Japan) scanning electron microscope (SEM) equipped with an energy dispersive X-ray microanalyzer (EDXA) INCA X-MAX by Oxford Instrument (Abingdon, UK) for the quantification of the elemental (chemical) composition of the samples within the range of 5 μm in diameter. An atomic-force microscope NTEGRA by NT-MDT (Zelenograd, Russia) was also used in our experiments. Prior to the measurements, glass bulbs were mechanically destroyed, and RS blades were extracted. No special cleaning or treatments of the contact surfaces were performed, except the removal of residual small glass pieces with a jet of pure nitrogen.

3. Results

Scanning electron microscopy (SEM) images of the cathode and anode coatings on the contact surface of RS blades were measured after the commutation tests with I_c of 0.4 A and 0.8 A for 10^6 switching cycles. In Figure 2 (I_c = 0.4 A), one can see the traces of planar and peak erosion in the form of disks on the cathode blade (Figure 2a) and respective craters (cups) on the anode blade (Figure 2b). The total area of these formations reached 1.3×10^{-2} mm^2. It was estimated from the SEM images with lower magnification (not shown here). Similar results were obtained for I_c = 0.8 A (Figure 3). In Figure 3, we also present the radial difference in the atomic concentration of nickel and iron measured by EDXA.

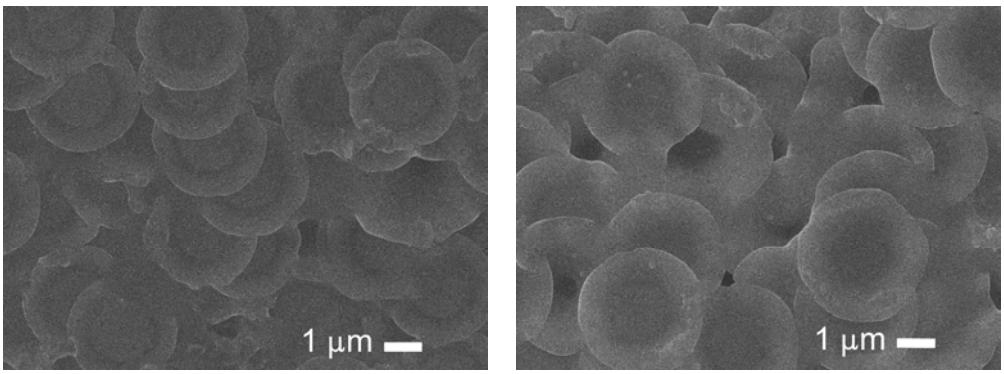

(**a**) (**b**)

Figure 2. SEM images measured for the coatings on the working surface of RS blades after the commutation test with I_c = 0.4 A and 10^6 switching cycles: (**a**) cathode; (**b**) anode.

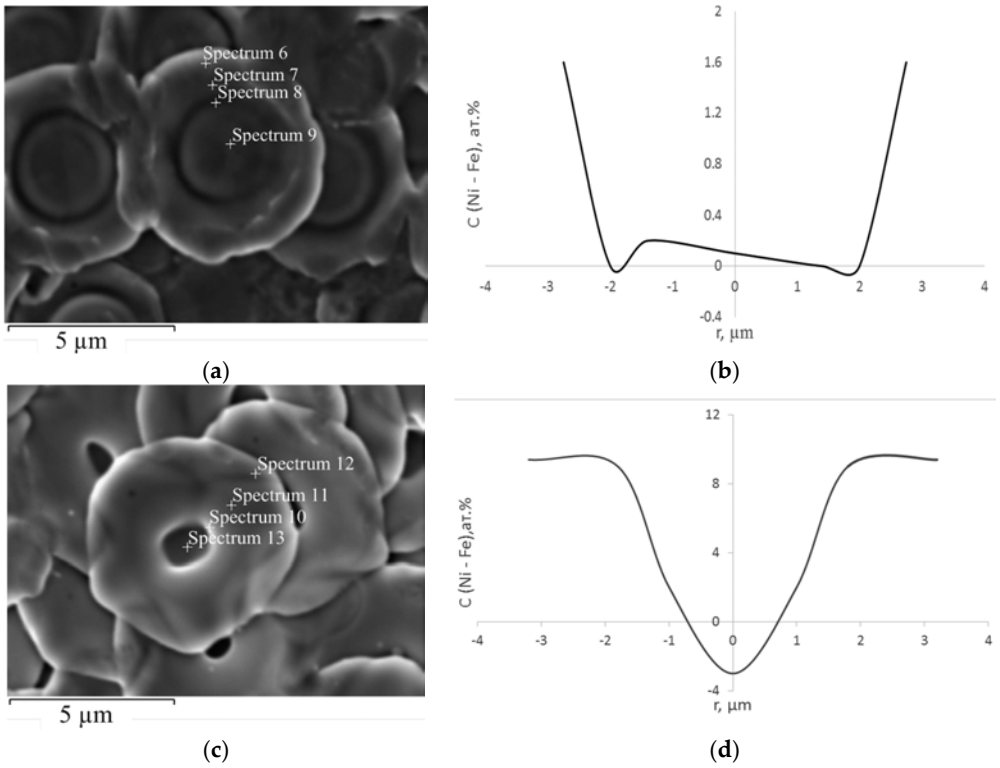

Figure 3. SEM images and energy dispersive X-ray microanalyzer (EDXA) distributions of the radial difference in the concentration of nickel and iron C (Ni-Fe) at % measured for the coatings on the working surface of RS blades after the commutation test with I_c = 0.8 A and 10^6 switching cycles: (**a**,**b**) cathode; (**c**,**d**) anode. Crosses and inscriptions on the SEM images indicate the position of EDXA measurements. The uncertainty of these measurements was not higher than 0.2 at %.

Cathode formations mainly consisted of similar-in-form and dimensions disk-like features produced by the transfer of anode materials (Figures 2a and 3a). As a result, a large quantity of small craters with fine structures is observed on the anode. They are located on the contrary of the cathode disks (Figures 2b and 3c). It should be noted that the diameters of the anode craters exceed the sizes of the cathode disks.

The Ni concentration increased when moving from the center to periphery for both the cathode disks (Figure 3b) and the anode craters (Figure 3d). However, this tendency was more pronounced for anode features.

Atomic-force microscopy (AFM) images and relief profiles of the anode and cathode features measured after the commutation test with I_c = 0.4 A and 10^6 switching cycles are presented in Figure 4. Similar holes are observed in the centers of each round features for both the cathode (Figure 4a,b) and for the anode (Figure 4c,d). However, the bottom of the cathode disks appears to be inhomogeneous, with humps, while the anode craters exhibit a rather smooth bottom.

We carried out similar measurements for I_c = 0.8 A and presented the geometrical characteristics (diameters, depths, and volumes) of these features versus the values of electric current for the cathode coatings in Table 1 and for the anode coatings in Table 2. The uncertainty of our measurements did not exceed 10%–15%. Proportionality between the values of geometrical characteristics and commutation currents was revealed for both types of the coatings.

We studied an influence of the numbers of switching cycles, N, on the surface morphology and atomic composition of the cathode and anode features for the commutation current I_c = 0.4 A. The N-value was changed sequentially each time by a factor of ten, starting from 10^3 (Figure 5a,b) and finishing at 10^6 (Figure 5c,d). The images obtained for the intermediate N-values are not shown here.

The following patterns were revealed from the experimental data acquired after the commutation tests with different numbers of switching cycles:

- the form and geometrical characteristics of the cathode disks and the anode craters were independent of N;
- the number of the cathode and anode features proportionally increased with N;
- the total erosion of the coatings on the working surface of the contacts after the commutation test possessed the resultant character—i.e., physicochemical specificities of erosion occurring after each commutation event were characteristic for the whole commutation test.

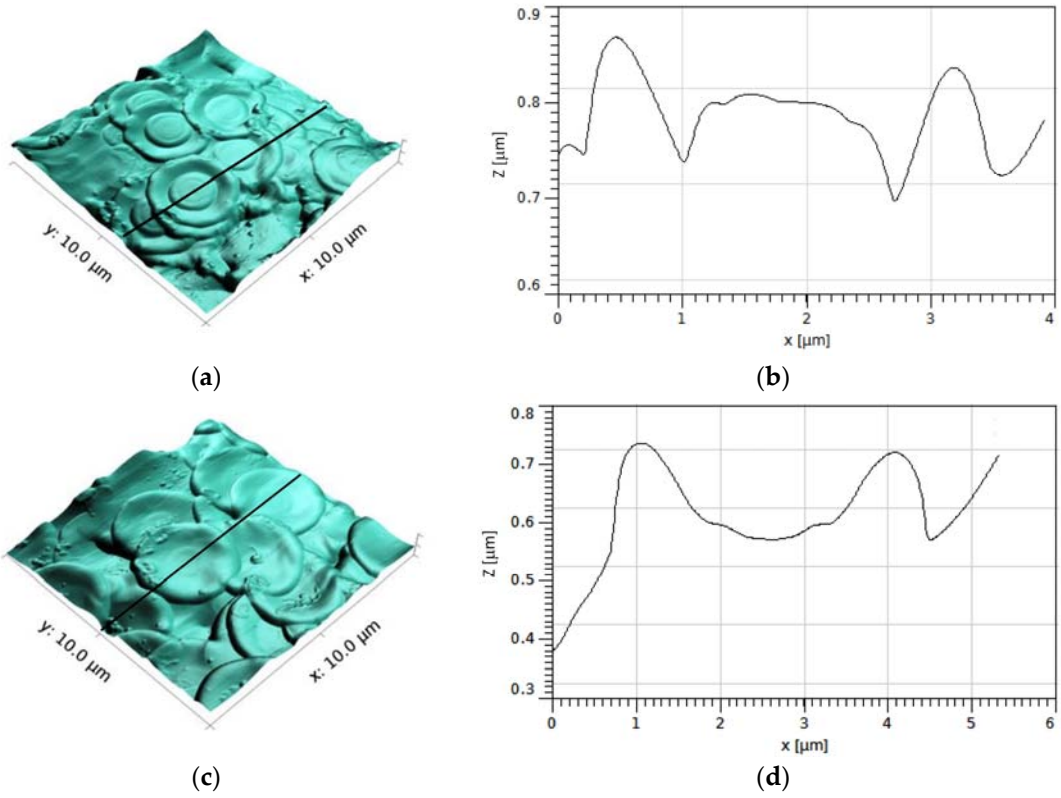

Figure 4. Atomic force microscopy (AFM) images and the relief profiles obtained for the coatings on the working surface of RS blades after the commutation test with I_c = 0.4 A and 10^6 switching cycles: (**a**,**b**) cathode; (**c**,**d**) anode. The relief profiles were measured along the lateral trace lines shown in panels (a,c).

Table 1. Geometrical characteristics of the cathode features versus the commutation current.

Commutation Current, A	Cathode Disks			Cathode Humps		
	Diameter, µm	Depth, µm	Volume, µm^3	Diameter, µm	Depth, µm	Volume, µm^3
0.4	2.8	0.12	0.4	1.7	0.05	0.11
0.8	5.0	0.25	8.5	2	0.1	0.31

Table 2. Geometrical characteristics of the anode craters versus the commutation current.

Commutation Current, A	Diameter, µm	Depth, µm	Volume, µm^3
0.4	3.0	0.15	0.36
0.8	6.0	1.0	9.42

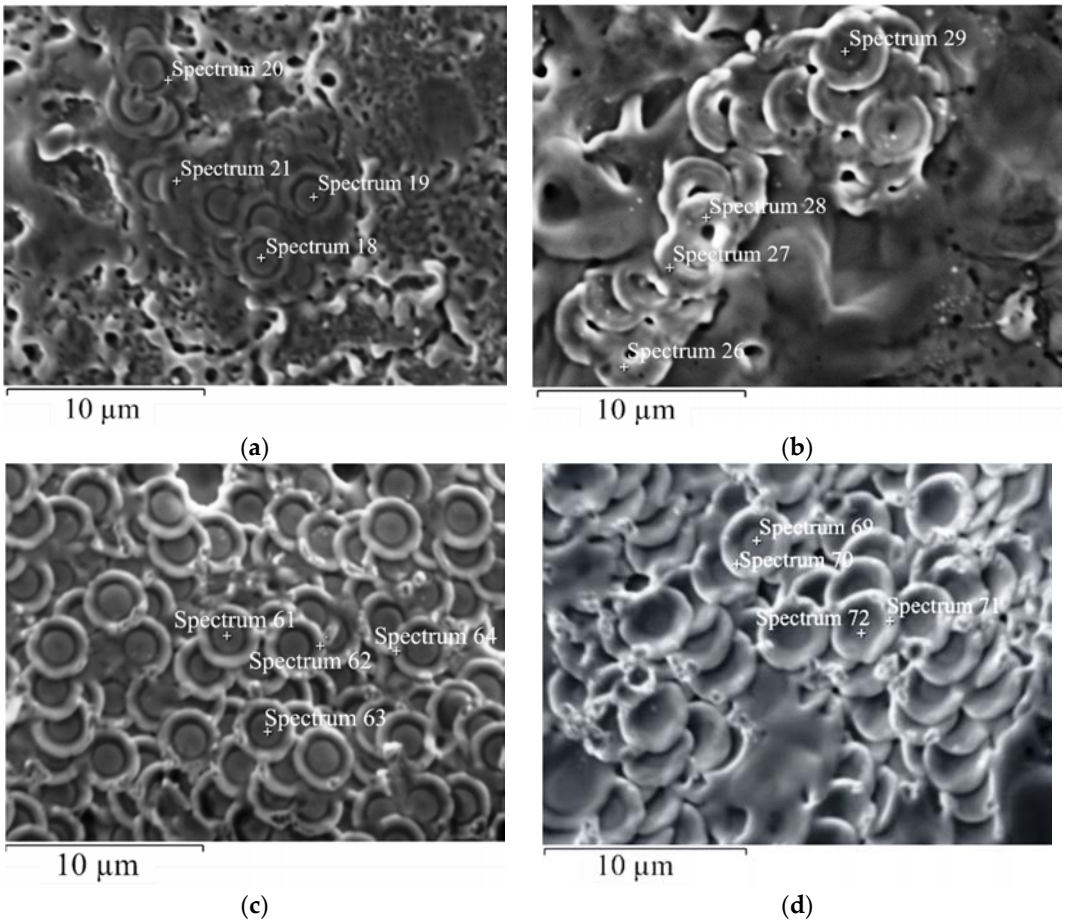

Figure 5. SEM images collected for the coatings on the working surface of RS blades after the commutation tests with I_c = 0.4 A and different numbers of switching cycles N: (**a**) cathode, $N = 10^3$; (**b**) anode, $N = 10^3$; (**c**) cathode, $N = 10^6$; (**d**) anode, $N = 10^6$. Crosses and inscriptions on the panels indicate the position of EDXA measurements.

4. Discussion

The commutation of electric current by reed switches begins from the mechanical approach of anode to cathode with the following electrical breakdown of the inter-electrode gap. As mentioned above, this process is in many respects similar to electrical discharge machining and doping (EDMP) [4,5]. According to the EDMP model developed by Lazarenko [4], an increase of the electric field in the course of approaching electrodes stimulates spark discharge between them. The breakdown path (channel) is formed, and the electron packets emitted from the cathode impact on the anode surface. As a result, the drops of molten metal formed on the anode surface leave it and move towards the cathode. During this movement, the metal drops get hot, begin to boil, and finally explode. Small parts of the exploded drops are deposited on the cathode surface and then crystallize. If the inter-electrode gap is filled by gas, gas molecules can also interact with the cathode surface. The amount of materials transferred from anode to cathode during the EDMP is proportional to the number of electrical discharges. This means that the total erosion of electrodes occurring in the course of electrical discharge and doping can be considered as a sum of single erosion events.

This discrete EDMP model is in a good agreement with the similar model of explosive electron emission (EEE) developed by Mesyats [2,3]. According to the EDMP model, the motive force of erosion, mass transfer, and portioning is the electron packet, and in the EEE model this role is assigned to the discrete electron avalanche named *ecton*.

Relying on the *ecton* concept, the dynamic of mass transfer of anode materials on the cathode surface is considered. An electrical potential of 24 V was applied to RS contacts during the commutation tests. This value is much lower than the breakdown voltage of the inter-electrode gap, which is equal to 280–290 V. Considering that the initial distance between contacts is d = 30 μm, one can estimate the initial electric field of 0.8×10^4 V·cm^{-1}. When the contacts start approaching, the electric field starts to increase and reaches 10^5–10^6 V·cm^{-1} at the distance of 0.1–1 μm. Moreover, on microirregularities (asperities), which usually exist on all surfaces, the electric field can increase up to 10^7–10^8 V·cm^{-1} [2,3].

Such d-values are comparable with the mean free path of electrons λ_e in gas atmosphere

$$\lambda_e = \frac{5.7kT}{\sqrt{2}\,\pi\delta^2 p} \quad (1)$$

where k is the Boltzmann constant, T is the gas temperature, δ is the diameter of a gas molecule, and p is the gas pressure. For T = 300 K, p = 39.96 kPa, and δ = 0.38 nm (nitrogen), λ_e can be estimated as 0.9 μm.

Under the previously stated experimental conditions, gas ionization via the Townsend electron avalanche mechanism cannot be realized, and the electrical breakdown can be initiated only by the field electron emission of a high density. Besides, the atomization and ionization of nitrogen resulting in the nitriding of contacts cannot occur. At the level of EDXA sensitivity, the presence of nitrogen was not detected in the erosion area of RS contacts, despite the fact that nitrogen concentration was 5–10 at % near the surface of the contacts. It should be noted that at higher electric voltages (50–100 V), when $d > \lambda_e$, simultaneously with the decomposition (decay) of the nitrogen-containing coatings, the process of their reduction takes place under the influence of nitrogen atoms and ions produced in a glass bulb of reed switches by spark discharges.

During the breakdown, when $d \leq 0.9$ μm, field and thermo-field electron emission initiates the electric current flowing inside the inter-electrode gap. When the density of this current reaches the threshold value of 10^8 A·cm^{-2}, the spark stage of discharge starts. At this stage, a great increase of the electric field—up to 10^8 V·cm^{-1}—induces explosive electron emission off of surface microirregularities. This results in the electrical explosion of the cathode, which is accompanied by the release of cathode materials in the form of solid, liquid, gaseous, and plasma fluxes. The drops of liquid metal move off the cathode to the anode at a speed of 10^4 cm·s^{-1}, and the plasma jet propagates with a speed of 10^6 cm·s^{-1}. According to [2], electrons in the jet possess zero-value work function, and they are ejected from it as discrete packets (*ectons*) with the mean velocity v_e ~10^8 cm·s^{-1}. The number of electrons in each *ecton* is estimated in the range of n_e ~10^{10}–10^{12}, and the time of *ecton* generation is ca. t_e ~10^{-8} s [2,3].

The temperature inside the breakdown channel can reach 10^4 °C, and the interaction of *ectons* with the anode surface results in its explosion, the generation of a plasma jet, drops of liquid metal, and crater production. The anode craters are larger than the cathode craters, because electrons from the anode jet return to the anode and additionally heat it. Besides, ions emitted from the anode compensate the space charge of electrons that increases the intensity of the explosive electron emission and still further heat the anode surface. The higher heating of the anode as compared to the cathode stimulates the directional mass transfer of the anode materials to the cathode. During this process, the anode plasma jet, drops, and vapors of the anode materials move inside the inter-electrode gap in the opposite direction of the cathode fluxes and interact with them. As a result, one or more asperities (humps) consisting of a large quantity of similar-in-form and dimensions disk-like features is produced on the cathode surface. On the anode surface, the same number of small craters located on the internal surface of the anode features is generated. The materials emitted from these craters by means of directional mass transfer contribute to the formation of the cathode humps (see Figures 2–4 and Tables 1 and 2).

In [4], the volume of the materials transferred from anode to cathode by spark pulse discharges is considered proportional to I^3. Our measurements of the volume of anode craters shown in Figure 4c,d gave the dependence

$$V = cI^{4.7} \quad (2)$$

where $c \approx 26.88$ μm^3·A$^{-4.7}$.

As shown in Table 2, the volumes of anode craters are 0.36 μm^3 and 9.42 μm^3 for the commutation currents 0.4 A and 0.8 A, respectively, and the volumes of the corresponding cathode disks are 0.4 μm^3 and 8.5 μm^3 (Table 1). These values are approximately equal pairwise (for the same values of the commutation current). Based on this parity, one can propose that the cathode disks were formed by materials transferred from the holes located in the anode craters. We estimated the value of kinetic energy E_e of *ecton*, which can produce such holes by affecting the anode surface. For $n_e = 10^{12}$ and $v_e \sim 10^8$ cm·s^{-1}, we obtained $E_e \sim 10^{-7}$ J. Similar values of the energy (0.96×10^{-7} J and 1.92×10^{-7} J for 0.4 A and 0.8 A, respectively) are transmitted to the small volume of the cathode. At the same time, much lower energy is needed for the sublimation of the above-mentioned volumes of anode materials (ca. 0.36×10^{-8} J and 9.42×10^{-8} J, respectively). This means that the main part of the explosion energy is spent on the ionization and transportation of the materials inside the inter-electrode gap and for *ecton* generation. The threshold energy of this process for anode and cathode made of iron can be estimated at the level of 10^{-8} J. Since $t_e = 10^{-8}$ s, the threshold power of an electric source which is able to initiate contact erosion in the frame of the *ecton* model should be greater than 1 W. In our experiments, this corresponds to the electric current $I_c > 0.04$ A. In fact, in the SEM images collected after the commutation tests with 0.04–0.05 A, no traces of contact surface erosion were observed.

Resting upon the experimental results, we suggest that the erosion stability of materials depends on the specific sublimation H_{sub} and ionization E_i energies of these materials. The criterion of erosion stability Z can be considered proportional to the sum of these energies

$$Z \propto H_{sub} + E_i \quad (3)$$

The electrospark resistance of materials was discussed in the Palatnik's theory [14,16,17], where the factor of electroerosion machinability M was introduced. The higher its value, the lower erosion stability of materials (Table 3).

Table 3. The experimental values of the factor M estimated for different metals [14].

Al	AISI 1044	Cu	Fe	Ni	Mo	W
1.5–1.7	1.0	1.3	0.9	0.9	0.8	0.7

In Table 4, we compare the relative values of the criterion of erosion stability Z with the reciprocal factor of electroerosion machinability M. Both Z and M values were normalized to the data for tungsten, as the most erosion-stable metal.

Table 4. Comparison of the erosion stability Z with the electroerosion machinability M for different metals.

Metal	H_{sub} *, kJ·mol^{-1}	E_i *, kJ·mol^{-1}	Z, kJ·mol^{-1}	Z/Z_W	M_W/M
Al	230.1	569.0	799.1	0.49	0.47
Cu	339.7	736.4	1076.1	0.66	0.54
Fe	393.3	753.1	1146.4	0.7	0.78
Ni	398.2	739	1137.2	0.69	0.78
Mo	669.5	707.1	1376.6	0.84	0.88
W	878.6	765.7	1644.3	1	1

* The data for the sublimation and ionization energies (the first ionization potential) were taken from [18].

One can see a good agreement between Z/Z_W and M_W/M values, which corroborates our erosion model of contact surfaces of low-current reed switches.

Under interruption of electrical current, the breaking of contacts does not occur simultaneously due to surface roughness and the presence of microirregularities. The main part of the electric current concentrates within limited-area surface spots. This causes them to melt, and the formation of liquid metal jumpers (bridges). The subsequent explosion of these bridges can generate *ecton*, which produces the erosion of the contacts by a similar way as during the closing of contacts.

The following processes can be initiated under an impact of *ecton* on the anode surface: (1) heating and melt of the surface layers; (2) generation of gas and plasma jets, formation and propagation of shock waves; (3) crater formation, sputter cleaning, and rapid surface recrystallization; (4) redistribution of surface materials, increasing of vacancies and dislocations, etc. The formation of the anode craters and then the cathode disks on the RS contact surfaces after the commutation tests is the resultant effect of these processes.

The redistribution of iron and nickel shown in Figure 3d for the anode features is mainly caused by high-temperature heating. Apparently, this rapid process can stimulate Ni segregation on the periphery of the anode craters due to the lower surface energy of Ni in comparison with Fe [18]. At the same time, the redistribution is less pronounced for the cathode features (Figure 3b) since the metal drops, vapor, and plasma fluxes produced under *ecton* impact on the anode surface and then taking part in the formation of the cathode disks should be enriched by iron due to the lower specific sublimation energies of Fe as against Ni [18].

5. Conclusions

The results of the present study provide a detailed description and explanation of crater and disks formation, mass transfer, and materials redistribution on the contact surface of reed switches during the commutation of electrical circuits with an active load. For that, the model of surface corrosion taking into account different processes occurring on the contact surfaces and inside the inter-electrode gap was proposed. According to this model based on the explosive electron emission theory, the erosion stability of the surface coatings depends on the specific sublimation and ionization energies (the ionization potential) of the materials forming the coatings. An increase of these energies can prevent the localization of erosion and its transition from planar to peak form, which rapidly destroys the surface coatings. In further development of our model, we suggest that a few monolayers of metals (or alloys) with low ionization potential deposited on the main coatings can improve the erosion stability of the contacts. This suggestion is in agreement with the ideas patented in [19]. The authors of this patent proposed to cover rhodium coatings by a thin film of easily-ionized materials such as thallium. The presence of this film forces the spark to change its position on the contact surface after each breaking/shorting cycle, resulting in the spark delocalization, uniformity of the mass transfer on the contact surfaces, and finally an increase in the number of switching cycles without the thorough destruction of the coatings.

Acknowledgments: This work was supported by the Ryazan Metal Ceramics Instrumentation Plant Joint Stock Company.

Author Contributions: Igor A. Zeltser and Evgeny N. Moos conceived and designed the experiments; Aleksey S. Karpov performed the commutation tests; Nikolay B. Rybin carried out SEM and EDXA measurements; Igor A. Zeltser, Evgeny N. Moos and Alexander B. Tolstoguzov discussed the data; Alexander B. Tolstoguzov and Igor A. Zeltser wrote the paper.

Conflicts of Interest: The authors declare no conflict of interest.

References

1. Karabanov, S.M.; Maizels, R.M.; Shoffa, V.N. *Magnetically Operated Contacts (Reed Switches) and Products on Their Basis*; Intellekt: Dolgoprudnyi, Russia, 2011; p. 480. (In Russian)
2. Mesyats, G.A. *Explosive Electron Emission*; Fizmatlit: Moscow, Russia, 2011; p. 280. (In Russian)

3. Mesyats, G.A.; Barengol'ts, S.A. Mechanism of anomalous ion generation in vacuum arcs. *Phys. Uspekhi* **2002**, *45*, 1001–1018. [CrossRef]
4. Lazarenko, B.R.; Lazarenko, N.I. *Physics of the Spark Method for Metal Processing*; TsBTI MEI: Moscow, Russia, 1946; p. 76. (In Russian)
5. Gitlevich, A.E.; Mikhailov, V.V.; Parkanskii, N.Y.; Revutsky, V.M. *Electro Spark Doping of Metal Surfaces*; Shtiintsa: Chisinau, Moldova, 1985; p. 196. (In Russian)
6. Arushanov, K.A.; Zeltser, I.A.; Karabanov, S.M.; Maizels, R.M.; Moos, E.N.; Tolstoguzov, A. Ion-induced surface modification of magnetically operated contacts. *Coatings* **2012**, *2*, 8–44. [CrossRef]
7. Tolstoguzov, A.B.; Drozdov, M.N.; Zeltser, I.A.; Arushanov, K.A.; Teodoro, O.M.N.D. Ion-plasma treatment of reed switch contacts: A study by time-of-flight secondary ion mass spectrometry. *J. Anal. Chem.* **2014**, *69*, 1245–1251. [CrossRef]
8. Arushanov, K.A.; Drozdov, M.N.; Karabanov, S.M.; Zeltser, I.A.; Tolstogouzov, A. TOF-SIMS study on surface modification of reed switch blades by pulsing nitrogen plasma. *Appl. Surf. Sci.* **2013**, *265*, 642–647. [CrossRef]
9. Zeltser, I.A.; Gurov, V.S.; Rybin, N.B.; Tolstogouzov, A.; Fu, D.J.; Kumar, P. Fabrication of nitrogen-containing coatings in reed switches by pulsed ion-plasma treatment. *J. Surf. Investig.* **2016**, *10*, 1106–1118. [CrossRef]
10. Starinskiy, S.V.; Shukhov, Y.G.; Bulgakov, A.V. Dynamics of pulsed laser ablation of gold in vacuum in the regime of nanostructured film synthesis. *Tech. Phys. Lett.* **2016**, *42*, 411–414. [CrossRef]
11. Bleicher, G.A.; Krivobokov, V.P. *Erosion of Solid Surface by Powerful Beams of Charged Particles*; Nauka: Novosibirsk, Russia, 2014; p. 248. (In Russian)
12. Volchenkova, R.A. Relationship between enthalpy and physical-mechanical and erosion characteristics of metals. *Ehlektron. Obrab. Materia.* **1973**, *4*, 58–62. (In Russian).
13. Verkhoturov, A.D. *Physical-Chemical Principles of Electrical Discharge Machining and Doping of Metal Surfaces*; Dal'nauka: Vladivostok, Russia, 1992; p. 175. (In Russian)
14. Palarnik, L.S. Phase transformation under electrical discharge machining of metals and an experience in the establishing of the criterion of observed interactions. *Doklady Akademii Nauk SSSR* **1935**, *89*, 425–433. (In Russian).
15. Rabkin, L.I.; Evgenova, I.N. *Magnetically Operated Hermetic Contacts (Construction, Properties, and Applications)*; Svyaz': Moscow, Russia, 1976; p. 104. (In Russian)
16. Artamonov, B.A.; Vishnitsky, A.L.; Volkov, Yu.S.; Glazkov, A.V. *Dimensional Electric Treatment of Metals*; Vihsshaya Shkola: Moscow, Russia, 1978; p. 336. (In Russian)
17. Livshits, A.L.; Kravets, A.T.; Rogachev, I.S.; Sosenko, A.B. *Electroerosion Treatment of Metals*; Mashinostroenie: Moscow, Russia, 1967; p. 295. (In Russian)
18. Kikoin, I.K. *Tables of Physical Values*; Atomizdat: Moscow, Russia, 1975; p. 1006. (In Russian)
19. Gerasimenko, V.A.; Fel'metzger, V.V.; Shrayner, Yu.A. Contact Coating of Magnetically Operated Hermetical Contacts. USSR Patent 1,718,283, 7 March 1992.

© 2017 by the authors. Licensee MDPI, Basel, Switzerland. This article is an open access article distributed under the terms and conditions of the Creative Commons Attribution (CC BY) license (http://creativecommons.org/licenses/by/4.0/).